Polyhedron 72 (2014) 140–146

Contents lists available at ScienceDirect

Polyhedron

journal homepage: www.elsevier.com/locate/poly

The first nickel(II) complexes of disubstituted diphenyldithiophosphates: Synthesis, spectroscopic, electrochemical, antifungal and single crystal X-ray analysis

Sandeep Kumar [a], Ruchi Khajuria [a], Vivek K. Gupta [b], Rajni Kant [b], Sushil K. Pandey [a,*]

[a] Department of Chemistry, University of Jammu, Jammu 180006, J & K, India
[b] X-ray Crystallographic Laboratory, Department of Physics and Electronics, University of Jammu, Jammu 180006, J & K, India

ARTICLE INFO

Article history:
Received 14 November 2013
Accepted 27 January 2014
Available online 12 February 2014

Keywords:
Diphenyldithiophosphate
Cyclic voltammetry
Single crystal X-ray
Antifungal

ABSTRACT

Five novel nickel(II) complexes of disubstituted diphenyldithiophosphates, $[\{(ArO)_2PS_2\}_2Ni]$ [Ar = 2,4-$(CH_3)_2C_6H_3$ (**1**), 2,5-$(CH_3)_2C_6H_3$ (**2**), 3,4-$(CH_3)_2C_6H_3$ (**3**), 3,5-$(CH_3)_2C_6H_3$ (**4**) and 4-Cl-3-$CH_3C_6H_3$ (**5**)], have been synthesized in aqueous medium and structurally characterized by IR, heteronuclear NMR (^1H, ^{13}C and ^{31}P) spectroscopic and single crystal X-ray analyses. Complexes **1** and **5** crystallize in the triclinic space group $P\bar{1}$, whereas complex **4** crystallizes in the monoclinic space group $P2_1/n$. In these complexes, the ligands are coordinated to the nickel ion as a bidentate chelating agent *via* the two thiolate sulfur atoms, leading to a spirocyclic system. Crystal structure determination of complexes **1**, **4** and **5** reveals that the complexes consist of mononuclear units with the nickel(II) ion coordinated in a bis-bidentate fashion with a distorted square planar coordination environment. A cyclic voltammetry experiment was used to probe the redox capabilities of complex **4**. The investigated complexes, along with the ligands, have been screened for *in vitro* antifungal activities against the fungus *Penicillium chrysogenum*.

1. Introduction

Nickel sulfur chemistry has received considerable attention as nickel compounds have proved to be potentially important in a diverse number of technical applications, such as paramagnetic antiferromagnetic phase-changing materials [1] and hydrodesulfurization catalysts [2]. Their electrochemical applications have been well established, which include electrochemical activation of freons [3]. The unique morphologies of nickel sulfides have encouraged the preparation of nanomaterials and their data storage ability has been employed in the production of various nanowires [4]. Nickel sorbents have been investigated for their capability to remove sulfur compounds in soil and coal gas [5]. On a biological front, they are key components of natural hydrogenase and are active promoters in current hydrotreating catalysts [6]. Nickel thiolate complexes have received special attention in recent years because sulfur-ligated nickel complexes mimic the [Fe–Ni]-hydrogenase active site and dimeric metal complexes based on nickel thiolate hydrides have been shown to be catalytically active for proton reduction [7]. Nickel complexes with *O,O′*-dialkyl/alkylene dithiophosphates have consistently retained interest over the last few decades [8–11]. These ligands exhibit versatile modes of coordination and are known to exist in bidentate and monodentate forms. However, nickel complexes with the analogous aromatic ligands have been less studied [12,13]. A survey of the literature confirms the importance of nickel complexes with thio ligands, where the main thrust of research has been on the preparation of complexes having varied applications in agriculture as pesticides [14], in lubrication engineering as antiwear and extreme pressure additives [15,16], in industry as antioxidants of polyolefines [17] and as catalyst stabilizers [18]. In continuation of our work on dithiophosphates [19–21], we report herein for the first time the synthesis, spectroscopic, electrochemical, antifungal and single crystal X-ray analysis of nickel(II) diphenyldithiophosphate complexes having disubstituted phenyl rings.

2. Experimental

2.1. Materials and instrumentation

All chemicals and solvents used in this study were of high purity. Solvents were distilled and dried using standard methods before use. Chloroform (Thomas Baker, b.p. 61 °C) was dried over P_2O_5. All the disubstituted phenols were procured from Sigma Aldrich and used without purification. The sodium salts of disubstituted *O,O′*-diphenyldithiophosphates, *i.e.* $\{(2,4\text{-}CH_3)_2C_6H_3O\}_2PS_2Na$,

* Corresponding author. Tel.: +91 9419147679.
E-mail address: kpsushil@rediffmail.com (S.K. Pandey).

http://dx.doi.org/10.1016/j.poly.2014.01.036
0277-5387/

$\{(2,5\text{-}CH_3)_2C_6H_3O\}_2PS_2Na$, $\{(3,4\text{-}CH_3)_2C_6H_3O\}_2PS_2Na$, $\{(3,5\text{-}CH_3)_2C_6H_3O\}_2PS_2Na$ and $(4\text{-Cl-}3\text{-}CH_3C_6H_3O)_2PS_2Na$, were synthesized according to a literature procedure for tolyldithiophosphates [21]. Moisture was carefully excluded for the synthesis of the ligands throughout the experimental manipulations using standard Schlenk techniques. Nickel was estimated gravimetrically as nickel(II)dimethylglyoximate. Chlorine was estimated by Volhard's method [22]. Elemental analyses (C, H, N and S) were conducted using an Elemental Analyser Vario EL-III (Indian Institute of Integrative Medicine, Jammu). Infrared spectra were recorded in the range 4000–200 cm^{-1} on a Perkin Elmer-spectrum RX1 FT-IR spectrophotometer (SAIF, Panjab University, Chandigarh). The ^1H and ^{13}C NMR spectra were recorded in $CDCl_3$ using TMS as an internal reference. The ^{31}P NMR spectra were recorded in $CDCl_3$ using H_3PO_4 (85%) as an external reference on a Bruker Avance III 400 MHz (Department of Chemistry, University of Jammu, Jammu). All chemical shifts are reported in δ units downfield from TMS = δ 0 ppm. The cyclic voltammogram was recorded on an Autolabs (Department of Chemistry, University of Jammu, Jammu). The potential was applied between the reference electrode (Ag/AgCl) and the working electrode (gold electrode) and the current was measured between the working electrode and the counter electrode (platinum wire). 0.1 M phosphate buffer solution (pH 7.0) was used. For antifungal studies, the fungus *Penicillium chrysogenum* was procured from the Department of Botany, University of Jammu, Jammu. All the glasswares and materials used for the antifungal activity measurements were sterilized in an autoclave.

2.2. Synthesis of complexes **1–5**

2.2.1. Synthesis of $[\{2,4\text{-}(CH_3)_2C_6H_3O\}_2PS_2]_2Ni$ (**1**)

To a stirred aqueous solution of $Ni(NO_3)_2{\cdot}6H_2O$ (0.40 g, 1.37 mmol), an aqueous solution of $\{(2,4\text{-}CH_3)_2C_6H_3O\}_2PS_2Na$ (1.00 g, 2.77 mmol) was added in a 1:2 M ratio with constant stirring. A solid precipitated immediately. After 30 min of stirring, the reaction contents were filtered to obtain the complex $[\{(2,4\text{-}CH_3)_2C_6H_3O\}_2PS_2]_2Ni$ (**1**) as a purple powdery solid. The complex was recrystallized from chloroform/*n*-hexane mixture (3:1) at room temperature. Yield: 0.91 g (91%); M.p. 172–174 °C (dec); *Anal.* Calc. for $C_{32}H_{36}O_4P_2S_4Ni$: C, 52.40; H, 4.95; S, 17.49; Ni, 8.00; Found: C, 52.35; H, 4.71; S, 17.47; Ni, 7.91%; IR (KBr, cm^{-1}): 1105 s [ν(P)–O–C], 869 s [νP–O–(C)], 650 s [$\nu P–S]_{asym}$, 572 m [$\nu P–S]_{sym}$, 370 w [νNi–S]; ^1H NMR ($CDCl_3$, ppm): 2.30 (s, 12H, 2–CH_3), 2.36 (s, 12H, 4–CH_3), 6.87 (d, J = 8 Hz, 4H, H_6), 7.07 (d, J = 8 Hz, 4H, H_5), 7.37 (s, 4H, H_3); ^{13}C NMR ($CDCl_3$, ppm): 17.3 (2–CH_3), 20.8 (4–CH_3), 120.8 (C_6), 127.4 (C_2–CH_3), 129.9 (C_5), 132.1 (C_4–CH_3), 135.4 (C_3), 146.8 (C_1–O); ^{31}P NMR ($CDCl_3$, ppm): 85.8 (s).

2.2.2. Synthesis of $[\{2,5\text{-}(CH_3)_2C_6H_3O\}_2PS_2]_2Ni$ (**2**)

Complex **2** was prepared by a similar procedure as described for complex **1**, using $Ni(NO_3)_2{\cdot}6H_2O$ (0.40 g, 1.37 mmol) and $\{(2,5\text{-}CH_3)_2C_6H_3O\}_2PS_2Na$ (1.00 g, 2.77 mmol). The resulting solid was recrystallized from a chloroform/*n*-hexane mixture (3:1) at room temperature. Yield: 0.89 g (89%); M.p. 180–182 °C (dec); *Anal.* Calc. for $C_{32}H_{36}O_4P_2S_4Ni$: C, 52.40; H, 4.95; S, 17.49; Ni, 8.00; Found: C, 52.36; H, 4.91; S, 17.42; Ni, 7.78%; IR (KBr, cm^{-1}): 1099 s [ν(P)–O–C], 876 s [νP–O–(C)], 653 s [$\nu P–S]_{asym}$, 578 m [$\nu P–S]_{sym}$, 372 w [νNi–S]; ^1H NMR ($CDCl_3$, ppm): 2.25 (s, 12H, 2–CH_3), 2.34 (s, 12H, 5–CH_3), 6.98 (d, J = 7.6 Hz, 4H, H_3), 7.12 (d, J = 7.6 Hz, 4H, H_4), 7.25 (s, 4H, H_6); ^{13}C NMR ($CDCl_3$, ppm): 16.6 (2–CH_3), 21.0 (5–CH_3), 121.6 (C_6), 126.1 (C_4), 127.0 (C_2–CH_3), 131.1 (C_3), 136.9 (C_5–CH_3), 149.4 (C_1–O); ^{31}P NMR ($CDCl_3$, ppm): 84.8 (s).

2.2.3. Synthesis of $[\{3,4\text{-}(CH_3)_2C_6H_3O\}_2PS_2]_2Ni$ (**3**)

Complex **3** was prepared by a similar procedure as described for complex **1**, using $Ni(NO_3)_2{\cdot}6H_2O$ (0.40 g, 1.37 mmol) and $\{(3,4\text{-}CH_3)_2C_6H_3O\}_2PS_2Na$ (1.00 g, 2.77 mmol). The resulting solid was recrystallized from a chloroform/*n*-hexane mixture (3:1) at room temperature. Yield: 0.90 g (90%); M.p. 169–171 °C (dec); *Anal.* Calc. for $C_{32}H_{36}O_4P_2S_4Ni$: C, 52.40; H, 4.95; S, 17.49; Ni, 8.00; Found: C, 52.33; H, 4.89; S, 17.46; Ni, 7.86%; IR (KBr, cm^{-1}): 1088 s [ν(P)–O–C], 861 s [νP–O–(C)], 653 s [$\nu P–S]_{asym}$, 573 m [$\nu P–S]_{sym}$, 368 w [νNi–S]; ^1H NMR ($CDCl_3$, ppm): 2.29 (s, 12H, 4–CH_3), 2.31 (s, 12H, 3–CH_3), 7.16 (d, J = 7.6 Hz, 4H, H_6), 7.28 (s, 4H, H_2), 7.40 (d, J = 8 Hz, 4H, H_5); ^{13}C NMR ($CDCl_3$, ppm): 19.2 (4–CH_3), 19.9 (3–CH_3), 118.3 (C_6), 122.2 (C_2), 130.4 (C_4–CH_3), 134.4 (C_5), 138.2 (C_3–CH_3), 147.8 (C_1–O); ^{31}P NMR ($CDCl_3$, ppm): 86.0 (s).

2.2.4. Synthesis of $[\{3,5\text{-}(CH_3)_2C_6H_3O\}_2PS_2]_2Ni$ (**4**)

Complex **4** was prepared by a similar procedure as described for complex **1**, using $Ni(NO_3)_2{\cdot}6H_2O$ (0.40 g, 1.37 mmol) and $\{(3,5\text{-}CH_3)_2C_6H_3O\}_2PS_2Na$ (1.00 g, 2.77 mmol). The resulting solid was recrystallized from a chloroform/*n*-hexane mixture (3:1) at room temperature. Yield: 0.92 g (92%); M.p. 187–189 °C (dec); *Anal.* Calc. for $C_{32}H_{36}O_4P_2S_4Ni$: C, 52.40; H, 4.95; S, 17.49; Ni, 8.00; Found: C, 52.32; H, 4.81; S, 17.43; Ni, 7.92%; IR (KBr, cm^{-1}): 1101 s [ν(P)–O–C], 858 s [νP–O–(C)], 654 s [$\nu P–S]_{asym}$, 557 m [$\nu P–S]_{sym}$, 371 w [νNi–S]; ^1H NMR ($CDCl_3$, ppm): 2.35 (s, 24H, 3,5–$(CH_3)_2$), 6.80 (s, 8H, $H_{2,6}$), 7.08 (s, 4H, H_4); ^{13}C NMR ($CDCl_3$, ppm): 21.3 (3,5–$(CH_3)_2$), 118.9 ($C_{2,6}$), 127.7 (C_4), 139.5 ($C_{3,5}$–CH_3), 149.6 (C_1–O); ^{31}P NMR ($CDCl_3$, ppm): 84.9 (s).

2.2.5. Synthesis of $[(4\text{-Cl-}3\text{-}CH_3C_6H_3O)_2PS_2]_2Ni$ (**5**)

Complex **5** was prepared by a similar procedure as described for complex **1**, using $Ni(NO_3)_2{\cdot}6H_2O$ (0.36 g, 1.24 mmol) and $(4\text{-Cl-}3\text{-}CH_3C_6H_3O)_2PS_2Na$ (1.00 g, 2.49 mmol). The resulting solid was recrystallized from a chloroform/*n*-hexane mixture (3:1) at room temperature. Yield: 0.90 g (90%); M.p. 144–146 °C (dec); *Anal.* Calc. for $C_{28}H_{24}O_4P_2S_4Cl_4Ni$: C, 41.25; H, 2.97; S, 15.73; Cl, 17.40; Ni, 7.20; Found: C, 41.16; H, 2.75; S, 15.54; Cl, 17.36; Ni, 7.09%; IR (KBr, cm^{-1}): 1157 s [ν(P)–O–C], 971 s [νP–O–(C)], 704 s [$\nu P–S]_{asym}$, 635 m [$\nu P–S]_{sym}$, 381 w [νNi–S]; ^1H NMR ($CDCl_3$, ppm): 2.27 (s, 24H, 3–CH_3), 7.13 (d, J = 8 Hz, 4H, H_6), 7.18 (s, 4H, H_2), 7.31 (d, J = 8.8 Hz, 4H, H_3); ^{13}C NMR ($CDCl_3$, ppm): 19.7 (3–CH_3), 120.6 (C_6), 123.9 (C_2), 127.1 (C_4–Cl), 128.7 (C_5–CH_3), 135.4 (C_3), 151.3 (C_1–O); ^{31}P NMR ($CDCl_3$, ppm): 86.1 (s).

All the complexes **1–5** were obtained as purple solids.

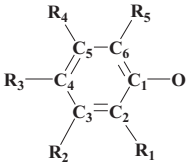

1. $\mathbf{R_1} = CH_3$, $\mathbf{R_2} = H_3$, $\mathbf{R_3} = CH_3$, $\mathbf{R_4} = H_5$, $\mathbf{R_5} = H_6$
2. $\mathbf{R_1} = CH_3$, $\mathbf{R_2} = H_3$, $\mathbf{R_3} = H_4$, $\mathbf{R_4} = CH_3$, $\mathbf{R_5} = H_6$
3. $\mathbf{R_1} = H_2$, $\mathbf{R_2} = CH_3$, $\mathbf{R_3} = CH_3$, $\mathbf{R_4} = H_5$, $\mathbf{R_5} = H_6$
4. $\mathbf{R_1} = H_2$, $\mathbf{R_2} = CH_3$, $\mathbf{R_3} = H_4$, $\mathbf{R_4} = CH_3$, $\mathbf{R_5} = H_6$
5. $\mathbf{R_1} = H_2$, $\mathbf{R_2} = CH_3$, $\mathbf{R_3} = Cl$, $\mathbf{R_4} = H_5$, $\mathbf{R_5} = H_6$

Scheme 1. Ring labelling for NMR spectroscopic assignments of complexes **1–5**.

2.3. Crystallography data collection and refinement

Crystallization of complexes **1**, **4** and **5** was executed by very slow evaporation of their saturated solutions in a chloroform/*n*-hexane mixture (3:1) at room temperature, yielding suitable single

Table 1
Summary of the crystal structure, data collection and structure refinement parameters for complexes **1**, **4** and **5**.

Complex	**1**	**4**	**5**
Crystal system	triclinic	monoclinic	triclinic
Space group	$P\bar{1}$	$P2_1/n$	$P\bar{1}$
Temperature, K	293(2)	293(2)	293(2)
Empirical formula	$C_{32}H_{36}NiO_4P_2S_4$	$C_{32}H_{36}NiO_4P_2S_4$	$C_{28}H_{24}Cl_4NiO_4P_2S_4$
Z	1	2	1
Formula weight	733.50	733.50	815.16
a (Å)	8.213(5)	13.4218(3)	7.1994(3)
b (Å)	9.317(5)	9.3238(2)	9.6421(3)
c (Å)	11.803(5)	13.8970(3)	13.0181(4)
α (°)	89.779(5)	90.00	87.660(3)
β (°)	76.444(5)	94.352(2)	76.108(3)
γ (°)	80.267(5)	90.00	74.335(3)
V (Å^3)	864.8(8)	1734.09(7)	844.39(5)
D_{calc} (g/cm^3)	1.408	1.405	1.603
$F(000)$	382	764	414
θ range for data collection (°)	3.47–26.00	3.66–25.99	3.75–26.00
No. of collected reflections	3400	3408	3303
No. of independent reflections	2429	2864	2904
R_{int}	0.0308	0.0490	0.0305
No. of data/restraints/parameters	3400/0/200	3408/0/200	3303/0/198
R_1, wR_2 [$I > 2\sigma(I)$]	0.0385, 0.0810	0.0336, 0.0832	0.0270, 0.0649
R_1, wR_2 (all data)	0.0624, 0.0913	0.0435, 0.0907	0.0328, 0.0684
Goodness-of-fit on F^2	0.986	1.063	1.031
Largest difference in peak/hole, (e Å^{-3})	0.309/−0.355	0.293/−0.358	0.324/−0.283

crystals for X-ray analysis. The structures of complexes **1**, **4** and **5** were determined by single crystal X-ray diffraction analysis. X-ray data of the complexes were collected on an X'calibur-Oxford Diffraction single crystal diffractometer with a CCD area-detector (graphite-monochromator, Mo Kα radiation, $\lambda = 0.71073$ Å). Data were corrected for Lorentz, polarization and absorption factors. The structures were solved by direct methods using SHELXS97 [23]. All non-H atoms of the molecules were located in the best E-map. Full-matrix least-squares refinement was carried out using SHELXL97 [23]. The geometry of the molecules were calculated using WinGX [24], PARST [25] and PLATON [26]. Atomic scattering factors were taken from the International Tables for X-ray Crystallography (1992, Vol. C, Tables 4.2.6.8 and 6.1.1.4). Molecular drawings were obtained using DIAMOND version 2.1 [27]. Crystallographic data and details of the data collection and structure solution and refinements are listed in Table 1.

2.4. Antifungal studies

An antifungal activity assay was carried out by the agar well diffusion method [28]. With a sterile cork borer of size 6 mm, 48 h old cultures grown on potato dextrose agar (PDA) were used for preparing the spore suspension for inoculation. 0.1 mL of the test fungal spore suspension was spread on sterile agar plates. Appropriate wells were made on the agar plate using the cork borer and 50 μL of test oil and fungicide of different concentrations were loaded. Plates were kept for pre-incubation for 30 min in a refrigerator and then were incubated for 48 h at 27 °C. The antifungal activity was evaluated by measuring the zone of inhibition of fungal growth surrounding the well with the sample solution in DMSO. The experiment was carried out in triplicate.

3. Results and discussion

The reactions of nickel(II) nitrate hexahydrate with sodium *O,O′*-bis(disubstitutedphenyl)phosphorodithioate in a 1:2 stoichiometric ratio were quite facile at room temperature and yielded the nickel(II) diphenydithiophosphates, formulated as [{$(ArO)_2PS_2$}$_2$Ni] [Ar = 2,4-$(CH_3)_2C_6H_3$ (**1**), 2,5-$(CH_3)_2C_6H_3$ (**2**), 3,4-$(CH_3)_2C_6H_3$ (**3**), 3,5-$(CH_3)_2C_6H_3$ (**4**) and 4-Cl-3-$CH_3C_6H_3$ (**5**)] according to Scheme 2. The precipitated purple solid complexes were separated by filtration and repeatedly washed with water. These complexes were found to be soluble in all common organic solvents.

3.1. IR spectra

The IR spectra of complexes **1–5** were recorded in the range 4000–200 cm^{-1} as KBr pellets and tentative assignments were made on the basis of relevant literature reports [11–13,21]. A comparison of the IR spectra of the complexes with the starting materials has also shown significant characteristic changes and shifting of the bands. Two strong intensity bands were observed in the regions 1157–1086 and 971–858 cm^{-1}, which may be ascribed to the [ν(P)–O–C] and [νP–O–(C)] vibrations of the diphenyldithiophosphate moiety, respectively. The bands for [νP–S]$_{asym}$ and [νP–S]$_{sym}$ of the diphenyldithiophosphate moiety were observed in the regions 704–653 and 635–557 cm^{-1}, respectively. The appearance of a new band for [νNi–S] in the region 381–368 cm^{-1} [13] in the spectra of these complexes is also indicative of the formation of a nickel–sulfur bond.

3.2. ^{1}H NMR

The ^{1}H NMR spectral data of complexes **1–5** show the characteristic proton resonances of the corresponding substituted phenyl protons. The splitting patterns of the peaks in the spectra of all the complexes were found to be consistent with the structures. The chemical shifts of the methyl ($-CH_3$) protons of the phenyl rings were observed as a singlet in the region 2.25–2.36 ppm. The aromatic protons of the phenyl groups were observed in the region 6.80–7.40 ppm with their characteristic splitting patterns. Three resonances were observed for the phenyl protons in complexes **1–3** and **5**, whereas complex **4** exhibited two resonances for the phenyl protons (Scheme 1).

3.3. ^{13}C NMR

The ^{13}C NMR spectra ($CDCl_3$) of complexes **1–5** showed that the chemical shifts due to the carbon atoms of the phenyl rings were retained with a marginal shift in their values compared to the parent ligands. The chemical shifts for the methyl ($-CH_3$) carbons attached to the phenyl rings were found in the region

$$2(ArO)_2PS_2Na + Ni(NO_3)_2.6H_2O \xrightarrow[\text{Stirring~30min}]{H_2O} [\{(ArO)_2PS_2\}_2Ni]$$
$$\text{-2NaNO}_3 \qquad \textbf{(1-5)}$$

Ar = 2,4-$(CH_3)_2C_6H_3$ (**1**), 2,5-$(CH_3)_2C_6H_3$ (**2**), 3,4-$(CH_3)_2C_6H_3$ (**3**), 3,5-$(CH_3)_2C_6H_3$ (**4**) and 4-Cl-3-$CH_3C_6H_3$ (**5**)

Scheme 2. Preparation of complexes **1–5**.

16.6–21.3 ppm. The carbon nuclei of the aryl groups displayed their resonances in the region 118.3–135.4 ppm. The chemical shifts for C–O carbon nuclei were found in the region 146.8–151.3 ppm. The chemical shifts for the C–(CH_3) carbon nuclei were observed in the region 127.0–139.5 ppm.

3.4. ^{31}P NMR

^{31}P NMR spectra of complexes **1–5** (proton-decoupled) showed the chemical shifts as a singlet in each case in the upfield region compared to the parent ligands (106.5–107.4 ppm), with a difference of 21–23 ppm. The phosphorus atom of the diphenyldithiophosphate moiety in the complexes shows one signal in the region 84.8–86.1 ppm, which is consistent with the bidentate behavior of the dithiophosphate moiety [29].

3.5. Crystal and molecular structures of complexes *1*, *4* and *5*

The X-ray diffraction analysis of complexes **1**, **4** and **5** reveals a monomeric distorted square planar geometry around the nickel centres (Figs. 1–3). Complexes **1** and **5** crystallize in the triclinic space group $P\bar{1}$, whereas complex **4** crystallizes in the monoclinic space group $P2_1/n$. The nickel atom is four coordinated by four sulfur atoms from two acyclic dithiophosphato ligands bonded in bidentate chelating fashion to form a spirocyclic ring. A selection of the bonds lengths and angles for complexes **1**, **4** and **5** are given in Table 2. The Ni–S1 and Ni–S2 bond distances are 2.229(11) and 2.229(11) Å for complex **1**, 2.2305(6) and 2.2370(6) Å for complex **4** and 2.2396(5) and 2.2438(5) Å for complex **5**, which are comparable to the values observed in the square-planar complex

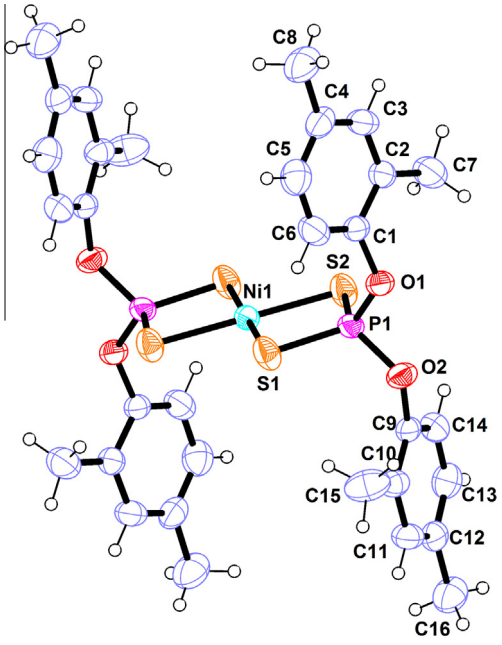

Fig. 1. Molecular structure of $[\{2,4\text{-}(CH_3)_2C_6H_3O\}_2PS_2]_2Ni$ (**1**) with displacement ellipsoids drawn at the 50% probability level.

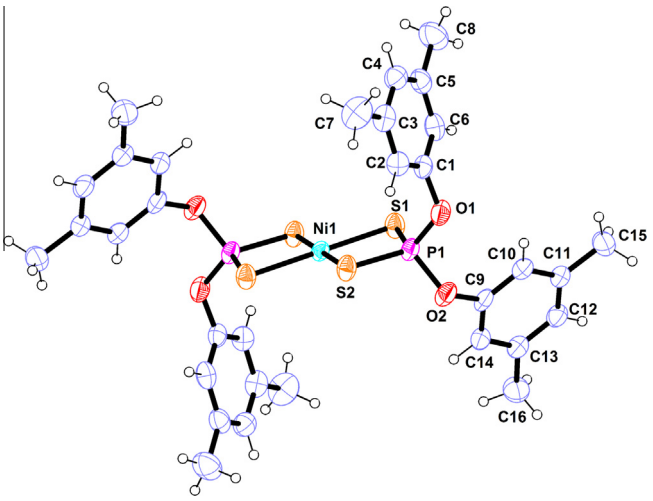

Fig. 2. Molecular structure of $[\{3,5\text{-}(CH_3)_2C_6H_3O\}_2PS_2]_2Ni$ (**4**) with displacement ellipsoids drawn at the 50% probability level.

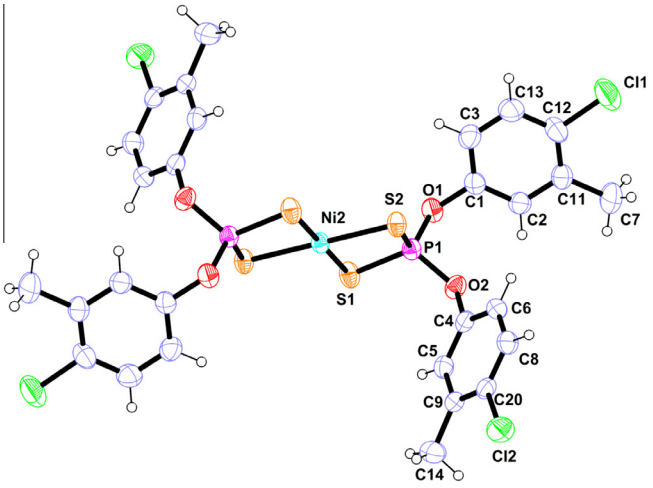

Fig. 3. Molecular structure of $[(4\text{-Cl-}3\text{-}CH_3C_6H_3O)_2PS_2]_2Ni$ (**5**) with displacement ellipsoids drawn at the 50% probability level.

$Ni[S_2P(OC_6H_4CH_3\text{-}o)_2]_2$ (2.2415(6) and 2.2241(6) Å) [12]. These bond lengths are also comparable to bond lengths of dialkyl dithiophosphate analogues reported in the literature, such as $Ni[S_2P(OBu^i)_2]_2$ (2.2244(5) and 2.2278(5) Å) [11], $Ni[S_2P(OEt)_2]_2$ (2.230 and 2.236 Å) [30] and $Ni[S_2P(OPr^i)_2]_2$ (2.227(1) and 2.216(1) Å) [31]. The P1–S1 bond distances are 1.984(13), 1.9778(8) and 1.9723(7) Å in complexes **1**, **4** and **5**, while the P1–S2 bond distances are 1.984(12), 1.9770(8) and 1.9776(7) Å, respectively. These bond distances are analogous to the values observed in $Ni[S_2P(OC_6H_4CH_3\text{-}o)_2]_2$ (1.9839(7) and 1.9850(7) Å) and $Ni[S_2P(OC_6H_4CH_3\text{-}m)_2]_2$ (1.9884(8) and 1.9778(8) Å) [12]. In the ditolyldithiophosphate derivative $Ni[S_2P(OC_6H_4Me\text{-}o)_2]_2\ C_{14}H_{12}N_2\ C_6H_6$ [13], the chelation of one of the dithiophosphato ligands is defined as (aniso)bidentate, in which the P1–S1 and P1–S2 bond

Table 2
Selected bonds lengths (Å) and angles (°) for complexes **1**, **4** and **5**.[a]

1			
Ni1–S1	2.229(11)	S1–Ni1–S2^{i}	91.96(4)
Ni1–S2	2.229(11)	S1–Ni1–S2	88.04(4)
S1–P1	1.984(13)	S1–P1–S2	102.65(5)
S2–P1	1.984(12)	S1–P1–O1	115.52(9)
P1–O1	1.583(18)	S1–P1–O2	115.74(9)
P1–O2	1.580(2)	S2–P1–O1	115.21(8)
S1–Ni1–S1^{i}	180.00(4)	S2–P1–O2	115.73(9)
S2–Ni1–S2^{i}	180.00(4)	O1–P1–O2	92.85(10)
4			
Ni1–S1	2.2305(6)	S1^{ii}–Ni1–S2	88.79(2)
Ni1–S2	2.2370(6)	S1–Ni1–S2	91.21(2)
P1–S1	1.9778(8)	O1–P1–S1	114.20(8)
P1–S2	1.9770(8)	O2–P1–S1	114.19(7)
P1–O1	1.5880(18)	O1–P1–S2^{ii}	115.02(7)
P1–O2	1.5813(17)	O2–P1–S2^{ii}	109.98(7)
S1–Ni1–S1^{ii}	180.00(3)	S2^{ii}–P1–S1	104.43(4)
S2–Ni1–S2^{ii}	180.00(18)	O2–P1–O1	99.34(9)
5			
Ni2–S1	2.2396(5)	S1–Ni2–S2	89.142(18)
Ni2–S2	2.2438(5)	S1–Ni2–S2^{ii}	90.86(18)
S1–P1	1.9723(7)	O1–P1–O2	98.78(8)
S2–P1	1.9776(7)	S2–P1–O2	113.95(6)
P1–O1	1.5855(14)	S2–P1–O1	115.38(6)
P1–O2	1.5917(14)	S1–P1–O2	114.37(6)
S1–Ni2–S1^{ii}	180.00(2)	S1–P1–O1	108.91(6)
S2–Ni2–S2^{ii}	180.00(2)	S1–P1–S2	105.61(3)

[a] Symmetry transformations used to generate equivalent atoms: (i) $-x, -y, -z$, (ii) $1-x, -y, -z$.

lengths are 1.997(2) and 1.969(2) Å, whereas the other dithiophosphato ligand is bonded in a monodentate fashion, for which the P2–S3 and P2–S4 bond distances are 1.995(2) and 1.941(2) Å. The phosphorus-sulfur bond lengths in complexes **1**, **4** and **5** fall between the bond lengths of P–S and P=S bonds, since the phosphorus-sulfur bond distances of complexes **1**, **4** and **5** are marginally shorter than the single P–S bonds found in [Ni($S_2P\{O\}OCH_2CH_2Ph$)(dppe)] (2.042(2) and 2.038(2) Å) [32] and larger than the P=S bond observed in $HS_2POCMe_2CMe_2O$ (1.923(2) Å) [33].

The S1–Ni–S2 bond angles of complexes **1**, **4** and **5** are found to be 88.04(4)°, 88.79(2)° and 89.142(18)°, respectively, which are typical of square planar complexes, such as Ni[$S_2P(OBu^i)_2]_2$ (88.389(16)°) [11], Ni[$S_2P(OC_6H_4CH_3$-*o*$)_2]_2$ (88.39(2)°) [12], Ni[$S_2P(OC_6H_4Me$-*p*$)_2]_2$ (89.12(2)°) [34], Ni[$S_2P(OEt)_2]_2$ (88.5°) and Ni[$S_2P(OPr^i)_2]_2$ (88.10(4)°). However, these bite angles are reduced to 82.05(4)° and 81.33(2)° in the adducts Ni[$S_2P(OC_6H_4Me$-*o*$)_2]_2$ $C_{14}H_{12}N_2$ C_6H_6 [13] and Ni[$S_2P(OC_6H_4Me$-*p*$)_2]_2$ $C_{10}H_8N$ [13], respectively. The distortion in the bond angles is obviously caused by the presence of the donor atom. The S1–P1–S2 bond angle for complex **1** is 102.65(5)°, which is akin to the values observed in Ni[$S_2P(OCH_2Ph)_2]_2$ (102.81(4)°) [12] and [Ni($S_2P\{OC_2H_5\}_2)_2$] (102.58(3)°) [35]. In complexes **4** and **5**, the S1–P1–S2 bond angles [104.43(4)° and 105.61(3)°] are quite analogous to the value found for Ni[$S_2P(OC_6H_4CH_3$-*m*$)_2]_2$ (104.18(4)°) [12]. So, a comparison of the data reveals that there are no significant changes in the bond distances and bond angles in alkyl-, tolyl- and diphenyl-dithiophosphate derivatives. The marginal difference in the values of the bond distances and angles may be attributed to the presence of a phenyl ring and any substitution on it.

3.6. Electrochemical behavior

The redox behavior of complex **4** in MeOH solution has been studied by cyclic voltammetry (Fig. 4). It clearly reveals that the redox process of the nickel(II) complex at the scan rate 100 mV/s involves a one step process with a reduction cathodic peak for the Ni(II)/Ni(I) couple at $E_{pc} = -0.27176$ V and with a peak current $I_{pc} = 1.45 \times 10^{-7}$ A. On the anodic side, the direct oxidation of Ni(I)/Ni(II) is observed at $E_{pa} = 0.62912$ V and the peak current is $I_{pa} = 1.60 \times 10^{-7}$ A. The difference between the cathodic and anodic potentials (ΔE_p) is −90 V. This couple is found to be quasi-reversible and the ratio of cathodic to anodic peak currents ($I_{pc}/I_{pa} = 0.90$) corresponds to a simple one-electron process. The $E_{1/2}$ value of the complex is +0.17 V.

3.7. Antifungal studies

Sulfur containing compounds are well known to exhibit antifungal activity [36]. Keeping this in view, the antifungal activities of the ligands and the representative metal complexes **1**, **4** and **5** have been measured against *P. chrysogenum*. The antifungal screening data (Table 3) establishes a linear relationship between concentration and zone of inhibition (in cm). On enhancing the concentration of the complex, the inhibition zone increases, *i.e.* all the complexes inhibited the growth of the fungus significantly. The ligands {(2,4-$CH_3)_2C_6H_3O\}_2PS_2Na$ (**L1**) and {(3,5-$CH_3)_2C_6H_3O\}_2$ PS_2Na (**L2**) showed a negligible inhibitory effect compared to the ligand (4-Cl-3-$CH_3C_6H_3O)_2PS_2Na$ (**L3**) and complexes **1**, **4** and **5**. This increase in activity of ligand **L3** may be due to the presence of a chloro group on the phenyl ring. Generally, the nature (electron withdrawing or electron releasing substituents) and position of the substituents present on the phenyl ring decide the antimicrobial activities. It is obvious that the inhibitory action becomes enhanced with the introduction of the electron-withdrawing chloro group on the phenyl ring [37]. Complexes **1**, **4** and **5** exhibit higher antifungal activities than the corresponding free ligands **L1**, **L2** and **L3** due to the chelation of the ligands with the nickel metal ion. It also reveals that an enhanced inhibitory effect of complex **5** is not only pertaining to the ligand **L3**, but chelation of the ligand with the nickel metal ion is also a liable factor. The increase in antifungal activity might be due to faster diffusion of the complexes as a whole through the cell membrane, or due to a combined activity effect of the metal and the ligand. The polarity of the metal ion will be reduced to a greater extent due to the overlap of the ligand orbitals and partial sharing of the positive charge of the metal ion with the donor group [38]. Further, it increases the delocalization of π-electrons over the whole chelate ring and enhances the

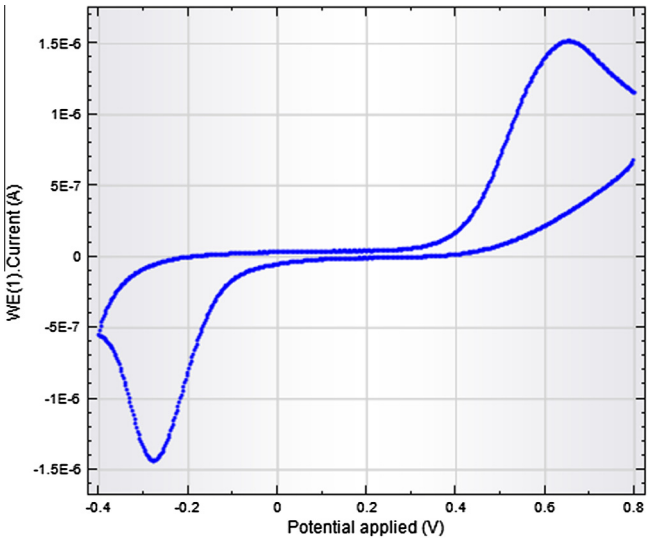

Fig. 4. Cyclic voltammetric curve of the complex [{3,5-$(CH_3)_2C_6H_3O\}_2PS_2]_2$Ni (**4**).

Table 3
Antifungal activity of the ligands and complexes against the fungus *Penicillium chrysogenum*.

Ligand/complex	Concentration (ppm)	Zone of Inhibition (in cm)
$\{(2,4\text{-}CH_3)_2C_6H_3O\}_2PS_2Na$ **(L1)**	100	0.0
	500	0.0
	1000	0.0
$\{(3,5\text{-}CH_3)_2C_6H_3O\}_2PS_2Na$ (**L2**)	100	0.0
	500	0.0
	1000	0.0
$(4\text{-}Cl\text{-}3\text{-}CH_3C_6H_3O)_2PS_2Na$ (**L3**)	100	0.5
	500	0.7
	1000	1.0
$[\{(2,4\text{-}CH_3)_2C_6H_3O\}_2PS_2]_2Ni$ (**1**)	100	0.4
	500	0.6
	1000	0.8
$[\{(3,5\text{-}CH_3)_2C_6H_3O\}_2PS_2]_2Ni$ (**4**)	100	0.4
	500	0.5
	1000	0.7
$[\{4\text{-}Cl\text{-}3\text{-}CH_3C_6H_3O\}_2PS_2]_2Ni$ (**5**)	100	0.8
	500	0.9
	1000	1.2

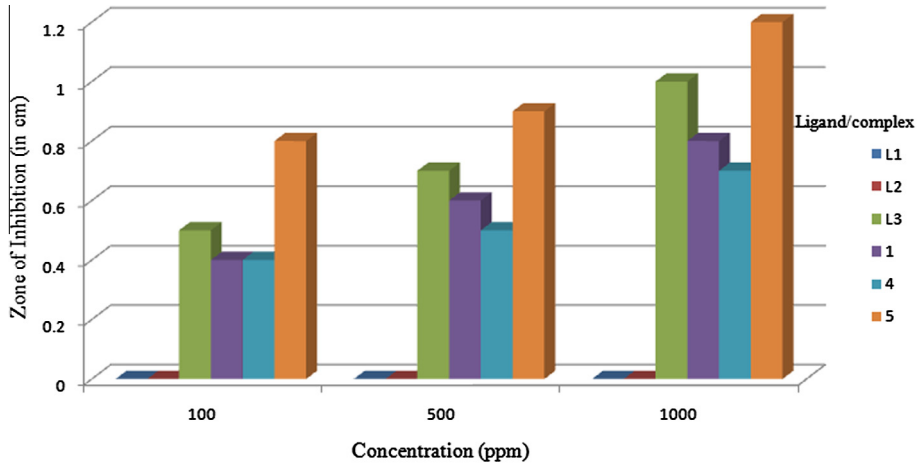

Fig. 5. Comparative results of antifungal screening data.

lipophilicity of the complexes, which enhances the penetration of the complexes into the lipid membranes and blocking of the metal binding sites in the enzymes of microorganisms, that restricts further growth of the organism. The fungal growth inhibition capacity of the complexes followed the order: **5** > **1** > **4**. The illustrated comparative results of antifungal analysis are given in Fig. 5.

4. Conclusion

We have reported the synthesis and characterization of some novel nickel(II) diphenyldithiophosphate complexes for the first time using a disubstituted phenyl ring having methyl and chlorine substituents. The results of the single crystal X-ray structure analysis establish the structural aspects of the new complexes. The elemental analysis, IR and NMR (^1H, ^{13}C and ^{31}P) results have been envisaged, on the basis of which a distorted square planar coordination environment is assigned around the nickel atom. Further, an electrochemical study depicted that the redox process is quasi-reversible and corresponds to a simple one-electron process. The antifungal screening of these complexes has indicated potential growth inhibition capacity in the order: **5** > **1** > **4**. The results are quite promising; hence these complexes are candidates for exploration as specific antifungal drugs due to their decent activity against *P. chrysogenum*.

Acknowledgments

The authors are grateful to the NMR laboratory Department of Chemistry, University of Jammu, Jammu for providing NMR spectral facilities (PURSE program). One of the authors (Rajni Kant) acknowledges the DST for the single crystal X-ray diffractometer as a National Facility under Project No. SR/S2/CMP-47/2003.

Appendix A. Supplementary material

CCDC 960922, 967391 and 967392 contain the supplementary crystallographic data for complexes **1**, **4** and **5**. These data can be obtained free of charge via http://www.ccdc.cam.ac.uk/conts/retrieving.html, or from the Cambridge Crystallographic Data Centre, 12 Union Road, Cambridge CB2 1EZ, UK; fax: (+44) 1223-336-033; e-mail: deposit@ccdc.cam.ac.uk.

References

[1] A. Olivas, J. Cruz-Reyes, V. Petranovskii, M. Avalos, S. Fuentes, J. Vac. Sci. Technol. A 16 (1998) 3515.
[2] W.J.J. Welters, G. Vorbeck, H.W. Zandbergen, J.W. Dehaan, V.H.J. Debeer, R.A. Vansanten, J. Catal. 150 (1994) 155.
[3] V.E. Titov, Y.D. Lampeka, A.M. Gatsun, I.M. Maloshtan, V.G. Koshechko, Theor. Exp. Chem. 37 (2001) 168.

[4] A.S. Samardak, E.V. Sukovatitsina, A.V. Ognev, L.A. Chebotkevich, R. Mahmoodi, S.M. Peighambari, M.G. Hosseini, F. Nasirpour, J. Phys. Conf. Ser. 345 (2012) 012011.
[5] J.H. Swisher, M. Jhunjhunwala, L.D. Gasper-Galvin, T.H. Gardne, K. Hammereck, J. Mater. Eng. Perform. 5 (1996) 247.
[6] D.A. Vicic, W.D. Jones, J. Am. Chem. Soc. 121 (1999) 4070.
[7] Z. Han, W.R. McNamara, M.S. Eum, P.L. Holland, R. Eisenberg, Angew. Chem., Int. Ed. 51 (2012) 1667.
[8] V. Machala, Z. Travnõcek, Z. Sindelar, L. Kvõtek, Transition Met. Chem. 25 (2000) 715.
[9] C.P. Bhasin, G. Srivastava, R.C. Mehrotra, Inorg. Chim. Acta 128 (1987) 69.
[10] C.P. Bhasin, R. Bohra, G. Srivastava, R.C. Mehrotra, P.B. Hitchcock, Inorg. Chim. Acta 164 (1989) 11.
[11] L. Bolundut, I. Haiduc, E. Ilyes, G. Kociok-Köhn, K.C. Molloy, S. Gómez-Ruiz, Inorg. Chim. Acta 363 (2010) 4319.
[12] A.L. Bingham, J.E. Drake, M.E. Light, M. Nirwan, R. Ratnani, Polyhedron 25 (2006) 945.
[13] A.L. Bingham, J.E. Drake, M.B. Hursthouse, M.E. Light, M. Nirwan, R. Ratnani, Polyhedron 26 (2007) 2672.
[14] P.E. Medyantseva, A.N. Ulakhovich, G.K. Budnikov, T.A. Groisberg, Zhurnal Analiticheskoi Khimii 46 (1991) 962.
[15] M. Born, J.C. Hipeaux, P. Marchand, G. Parc, Lubr. Sci. 4 (1992) 93.
[16] P.I. Sanin, Rev. Inst. Franc. Petrole, et Ann. Combustibles Liquids 16 (1961) 468.
[17] S. Al-Malaika, M. Coker, G. Scott, Polym. Degrad. Stab. 22 (1988) 147.
[18] F.A. Nasirov, Iran. Polym. J. 12 (2003) 281.
[19] A. Syed, S.K. Pandey, Monatsh. Chem. 144 (2013) 1129.
[20] S.C. Bajia, J.E. Drake, M.E. Light, M. Nirwan, S.K. Pandey, R. Ratnani, Polyhedron 28 (2009) 85.
[21] A. Kumar, K.R. Sharma, S.K. Pandey, Phosphorus, Sulfur Silicon Relat. Elem. 182 (2007) 1023.
[22] A.I. Vogel, A Textbook of Quantitative Inorganic Analysis, forth ed., Longman, London, 1978.
[23] G.M. Sheldrick, Acta Crystallogr., Sect. A 64 (2008) 112.
[24] L.J. Farrugia, J. Appl. Crystallogr. 32 (1999) 837.
[25] M. Nardelli, J. Appl. Crystallogr. 28 (1995) 659.
[26] A.L. Spek, Acta Crystallogr., Sect. D 65 (2009) 148.
[27] K. Brandenburg, DIAMOND, Version 2.1. Crystal Impact GbR, Bonn, Germany, 1998.
[28] D.P. Singh, V. Malik, R. Kumar, K. Kumar, J. Serb. Chem. Soc. 75 (2010) 763.
[29] C. Glidewell, Inorg. Chim. Acta 25 (1977) 159.
[30] J.F. McConnell, V. Kastalsky, Acta Crystallogr. 22 (1967) 853.
[31] B.F. Hoskins, E.R.T. Tiekink, Acta Crystallogr., Sect. C 41 (1985) 322.
[32] Y.-L. Li, B. Xie, L.-K. Zou, X. Lin, Y. Yang, S. Zhu, T. Wang, Polyhedron 67 (2014) 490.
[33] J.E. Drake, L.N. Khasrou, A.G. Mislankar, R. Ratnani, Polyhedron 19 (2000) 407.
[34] S.-S. Zhang, B. Yang, Y.-F. Wang, X.-M. Li, K. Jiao, M.B. Kassim, B.M. Yamin, Acta Crystallogr., Sect. E 60 (2004) 485.
[35] D. Paliwoda, J. Chojnacki, A. Mietlarek-Kropidłowska, B. Becker, Acta Crystallogr., Sect. E 65 (2009) 662.
[36] S. Kim, R. Kubec, R.A. Musah, J. Ethnopharmacol. 104 (2006) 188.
[37] N. Raman, J. Joseph, A. Sakthivel, R. Jeyamurugan, J. Chil. Chem. Soc. 54 (2009) 354.
[38] B.G. Tweedy, C. Loeppky, Phytopathology 58 (1968) 1522.